Dalton Transactions

Accepted Manuscript

This article can be cited before page numbers have been issued, to do this please use: M. Zain Aldin, A. MAHO, G. Zaragoza, A. Demonceau and L. Delaude, *Dalton Trans.*, 2018, DOI: 10.1039/C8DT02838A.

ROYAL SOCIETY OF CHEMISTRY

rsc.li/dalton

View Article Online
DOI: 10.1039/C8DT02838A

Dalton Transactions

ARTICLE

Synthesis, characterization, and catalytic evaluation of ruthenium–diphosphine complexes bearing xanthate ligands†

Received 00th January 20xx,
Accepted 00th January 20xx

DOI: 10.1039/x0xx00000x

www.rsc.org/

Mohammed Zain Aldin,[a] Anthony Maho,[b] Guillermo Zaragoza,[c] Albert Demonceau,[a] and Lionel Delaude*[a]

The reaction of $[RuCl_2(p\text{-cymene})]_2$ with potassium *O*-ethylxanthate and a set of nine representative $Ph_2P–X–PPh_2$ bidentate phosphines (dppm, dppe, dppp, dppb, dpppe, dppen, dppbz, dppf, DPEphos) afforded monometallic $[Ru(S_2COEt)_2(diphos)]$ chelates **1–9** in 62–96% yield. All the products were fully characterized by using various analytical techniques and their molecular structures were determined by X-ray crystallography. They featured a highly distorted octahedral geometry with a S–Ru–S bite angle close to 72° and P–Ru–P angles comprised between 73° and 103°. Bond lengths and IR stretching frequencies recorded for the anionic xanthate ligands strongly suggested a significant contribution of the $EtO^+{=}CS_2^{2-}$ resonance form. ^{1}H NMR and XRD analyses showed that the methylene protons of the ethyl groups were diastereotopic due to a strong locking of their conformation by a neighboring phenyl ring. On cyclic voltammetry, quasi-reversible waves were observed for the Ru^{2+}/Ru^{3+} redox couples with $E_{1/2}$ values comprised between 0.65 and 0.80 V *vs.* Ag/AgCl. The activity of chelates **1–9** was probed in three catalytic processes, *viz.*, the synthesis of vinyl esters from benzoic acid and 1-hexyne, the cyclopropanation of styrene with ethyl diazoacetate, and the atom transfer radical addition of carbon tetrachloride and methyl methacrylate. In the first case, ^{31}P NMR analysis of the reaction mixtures showed that the starting complexes remained mostly unaltered, despite the harsh thermal treatment that was applied to them. In the second case, monitoring the rate of nitrogen evolution revealed that all the catalysts under investigation behaved similarly and were rather slow initiators. In the third case, $[Ru(S_2COEt)_2(dppm)]$ was singled out as a very active and selective catalyst already at 140 °C, whereas most of the other complexes resisted degradation up to 160 °C and were only moderately active. Altogether, these results were in line with the high stability displayed by $[Ru(S_2COEt)_2(diphos)]$ chelates **1–9**.

Introduction

Since 2009, our Laboratory has been investigating the synthesis, characterization, and complexation of azolium-2-dithiocarboxylate betaines.[1,2] These stable, crystalline inner salts are the adducts of N-heterocyclic carbenes (NHCs) and carbon disulfide (Chart 1).[3] They form strong M–S bonds with a wide range of metals through various binding modes.[4] As a result, NHC·CS_2 zwitterions are particularly attractive for designing new molecular architectures based on transition metals.[5] Our first venture in this area focused on ruthenium–arene complexes containing imidazol(in)ium-2-dithiocarboxylate ligands.[2] Subsequent research efforts carried out in collaboration with the group of Wilton-Ely at Imperial College allowed to extend the coordination chemistry of these 1,1-dithiolate inner salts to osmium,[6] palladium,[7] and gold complexes.[8] More recently, we also reported the formation of mono- and bimetallic metal–carbonyl compounds based on manganese[9] and rhenium[10] that featured chelating or bridging NHC·CS_2 ligands, while Neuba and Wilhelm used these sulfur donors to assemble sophisticated copper coordination polymers and clusters.[11]

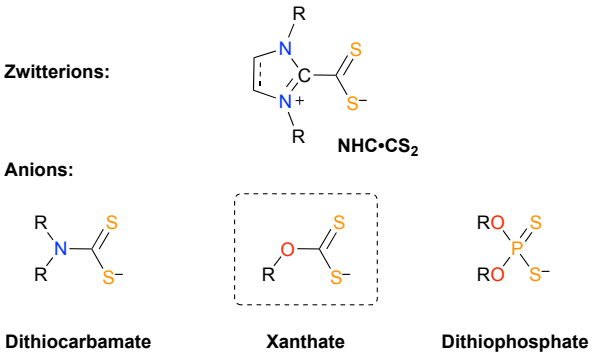

Chart 1 Generic structures of common 1,1-dithiolate ligands.

[a] *Laboratory of Catalysis, Institut de Chimie (B6a), Allée du six Août 13, Quartier Agora, Université de Liège, 4000 Liège, Belgium. E-mail: l.delaude@ulg.ac.be; http://www.cata.ulg.ac.be*
[b] *GreenMAT, Institut de Chimie (B6a), Allée du six Août 13, Quartier Agora, Université de Liège, 4000 Liège, Belgium*
[c] *Unidade de Difracción de Raios X, RIAIDT, Universidade de Santiago de Compostela, Campus Vida, 15782 Santiago de Compostela, Spain*

† Electronic Supplementary Information (ESI) available: ^{1}H, ^{13}C, and ^{31}P NMR spectra, IR spectra, and HR-MS spectra of compounds **1–9**, additional experimental details for XRD, CV, and catalytic tests. CCDC 1854853–1854861. For ESI and crystallographic data in CIF or other electronic format see DOI: 10.1039/x0xx00000x

Apart from azolium-2-dithiocarboxylate zwitterions, other related species, such as the dithiocarbamate,[12] dithiophosphate,[13] and xanthate anions,[14] have long dominated the coordination chemistry of 1,1-dithiolate ligands (Chart 1).[15] In particular, the last-mentioned oxygen-containing derivatives have been known for more than two centuries. Indeed, the term xanthate was coined by Zeise in 1822 to reflect the yellow appearance of various complexes bearing these ligands,[16] which should be more rigorously named *O*-alkyl (or aryl) dithiocarbonate anions. Over the years, xanthate salts have been widely used as flotation collectors in the mining and metallurgy of non ferrous metal sulfides.[17] They have also been employed as reagents in analytical chemistry[18] and to generate radical species in organic synthesis.[19] Contrastingly, their use as ancillary ligands in homogeneous catalysis is barely documented, with only a single report describing the electrocatalytic activity of a ruthenium–xanthate complex in tryptophan oxidation.[20]

In light of our sustained interest for ruthenium catalysts[21] and azolium-2-dithiocarboxylate zwitterions,[3] we decided to have a fresh look at the coordination chemistry of Ru(II) and xanthate ligands in view of potential catalytic applications. In this contribution, we report on the synthesis and full characterization of nine ruthenium–diphosphine complexes bearing *O*-ethyl dithiocarbonate ligands using efficient and straightforward synthetic protocols combined with modern analytical techniques. We also investigated the redox properties of the [Ru(S_2COEt)$_2$(diphos)] chelates obtained by cyclic voltammetry and we probed their catalytic activity in the synthesis of vinyl esters, in the cyclopropanation of styrene, and for atom transfer radical additions.

Results and discussion

Synthesis of [Ru(S_2COEt)$_2$(diphos)] complexes

In 1969, Wilkinson and coworkers first reported the synthesis of *cis*-[Ru(S_2COR)$_2$(PPh_3)$_2$] complexes (R = Me, Et) by reacting [$RuCl_2$(PPh_3)$_3$] with either potassium *O*-methylxanthate or potassium *O*-ethylxanthate in refluxing acetone for 12 h.[22] In 1975, Critchlow and Robinson showed that [RuH(OAc)(PPh_3)$_3$] was also a suitable starting material for this reaction[23] and in 1990 Chakravorty *et al.* noted that the use of refluxing ethanol in place of acetone significantly reduced its duration.[24] Subsequent work from Ballester and coworkers showed that [Ru(S_2COEt)$_2$(PPh_3)$_2$] reacted with tertiary mono- and diphosphines to afford [Ru(S_2COEt)$_2$(PR_2R')$_2$] (R_2R' = Ph_2Me, PH_2Et, or Me_2Ph) and [Ru(S_2COEt)$_2$($Ph_2P(CH_2)_xPPh_2$)] (x = 1, 2) complexes.[25]

To shorten the two-step procedure employed so far, our strategy to access [Ru(S_2COEt)$_2$(diphos)] complexes involved the one-pot chelation of both a diphosphine and two *O*-ethylxanthate ligands onto a ruthenium(II) center. For this purpose, we elected the readily available [$RuCl_2$(*p*-cymene)]$_2$ dimer (*p*-cymene is 1-isopropyl-4-methylbenzene) as the metal source, in combination with KS_2COEt and a set of nine representative bidentate phosphines with the generic formula Ph_2P–X–PPh_2. More specifically, our assortment comprised 1,1-bis(diphenylphosphino)methane (dppm), 1,2-bis(diphenylphosphino)ethane (dppe), 1,3-bis(diphenylphosphino)propane (dppp), 1,4-bis(diphenylphosphino)butane (dppb), 1,5-bis(diphenylphosphino)pentane (dpppe), *cis*-1,2-bis(diphenylphosphino)ethene (dppen), 1,2-bis(diphenylphosphino)benzene (dppbz), 1,1'-bis(diphenylphosphino)ferrocene (dppf), and 2,2'-bis(diphenylphosphino)diphenyl ether (DPEphos) (Chart 2).

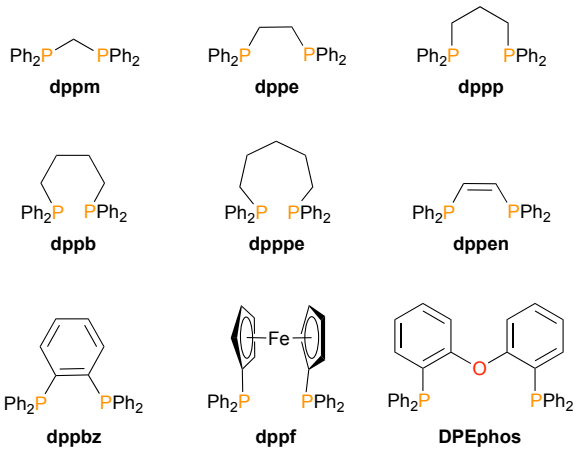

Chart 2 Diphosphine ligands used in this work.

In a typical experiment, the [$RuCl_2$(*p*-cymene)]$_2$ dimer (1 equiv.) and small excesses of Ph_2P–X–PPh_2 (2.2 equiv.) and KS_2COEt (4.4 equiv.) were stirred in THF for 24 h at room temperature. The resulting suspensions that possibly contained diphosphine-bridged multimetallic ruthenium–arene oligomers were then heated to induce the formation of the thermodynamically more stable monometallic [Ru(S_2COEt)$_2$(diphos)] chelates **1**–**9** (Scheme 1). This thermal treatment was required to achieve high yields of pure products. It was initially carried out by heating Schlenk flasks in an oil bath at 80–90 °C for 24 h. Alternatively, we also performed syntheses using a monomodal microwave reactor or a pressure reactor. With these equipments, THF could be heated up to 130 °C and completion was reached within 1 h. With dppe and dppb, precipitates that formed at room temperature remained insoluble even when the temperature was increased to 130 °C, thereby affording low yields of final products **2** and **4**. In these cases, we obtained better results by reacting first the [$RuCl_2$(*p*-cymene)]$_2$ dimer with potassium *O*-ethylxanthate for 24 h at room temperature before adding the diphosphine ligand and heating the mixture for 1 h at 130 °C. With this modification of the standard procedure, all the compounds **1**–**9** were isolated in satisfactory to excellent yields after a work-up to remove the various byproducts and excess reagents.

View Article Online
DOI: 10.1039/C8DT02879A

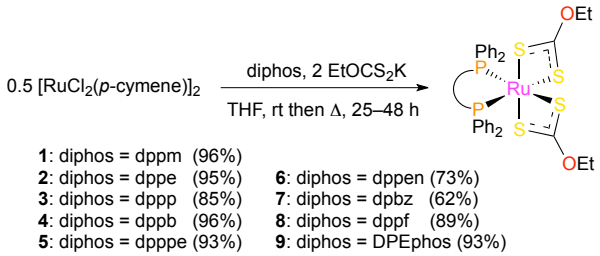

1: diphos = dppm (96%)
2: diphos = dppe (95%)
3: diphos = dppp (85%)
4: diphos = dppb (96%)
5: diphos = dpppe (93%)
6: diphos = dppen (73%)
7: diphos = dpbz (62%)
8: diphos = dppf (89%)
9: diphos = DPEphos (93%)

Scheme 1 Synthesis of $[Ru(S_2COEt)_2(diphos)]$ complexes **1–9**.

Structural analysis

^1H and ^{13}C NMR analysis of $[Ru(S_2COEt)_2(diphos)]$ chelates **1–9** provided evidence for the dissociation of *p*-cymene from the starting ruthenium dimer and for the incorporation of diphosphine and *O*-ethylxanthate ligands in 1:2 stoichiometric proportions. Strikingly, the methylene protons of the latter anionic moiety afforded either a complex multiplet or two distinct multiplets centered around 4 ppm on ^1H NMR spectroscopy. This pattern sharply contrasted with the usual quartet displayed by the OCH_2CH_3 group in KS_2COEt and in various organic xanthates with the generic formula RS_2COEt.[26] It is a sign of restricted rotation around the $CH_3CH_2–OCS_2^-$ bond leading to diastereotopic methylene protons, as further evidenced by X-ray crystallography (*vide infra*). The neighboring methyl group was not affected and resonated as a triplet around 1.2 ppm as expected. On ^{13}C NMR spectroscopy, the dithiocarboxylate unit led to a highly deshielded singlet at *ca.* 226 ppm (Table 1). This characteristic signal was only slightly shifted to lower field upon complexation (δ CS_2 = 230.3 ppm for KS_2COEt in DMSO-d_6). It was no further affected by varying the nature of the diphosphine ligand. These observations are in line with previous trends evidenced while studying the coordination chemistry of azolium-2-dithiocarboxylate zwitterions and other 1,1-dithiolate ligands.[6–15]

Table 1 ^{13}C NMR chemical shift of the CS_2 group and ^{31}P NMR chemical shift of the diphos ligand in $[Ru(S_2COEt)_2(diphos)]$ chelates **1–9** in $CDCl_3$ at 298 K

Complex	δ CS_2 (ppm)	δ P (ppm)
$[Ru(S_2COEt)_2(dppm)]$ (**1**)	226.5	3.34
$[Ru(S_2COEt)_2(dppe)]$ (**2**)	226.5	76.61
$[Ru(S_2COEt)_2(dppp)]$ (**3**)	226.6[a]	37.17[a]
$[Ru(S_2COEt)_2(dppb)]$ (**4**)	226.2	48.18
$[Ru(S_2COEt)_2(dpppe)]$ (**5**)	225.7	43.57
$[Ru(S_2COEt)_2(dppen]$ (**6**)	226.5	80.83
$[Ru(S_2COEt)_2(dppbz)]$ (**7**)	226.4	78.39
$[Ru(S_2COEt)_2(dppf)]$ (**8**)	225.0	46.68
$[Ru(S_2COEt)_2(DPEphos)]$ (**9**)	224.9	43.45

[a] Data recorded in CD_2Cl_2.

The ^{31}P NMR spectra of complexes **1–9** recorded in $CDCl_3$ or CD_2Cl_2 were particularly simple and neat, with only a single resonance present in all cases (Table 1). These data indicate a symmetrical chelation of the metal center by the diphosphine ligands. The chemical shifts observed were in line with those reported previously for other types of Ru(diphos) species.[27] As anticipated, the nature and the length of the spacer between the two phosphorus atoms had a profound influence on the magnetic properties of these nuclei. Indeed, when a bidentate phosphine is coordinated to a transition metal, the size and the topology of the metallacycle are known to induce significant variations in the ^{31}P NMR chemical shifts.[28] Of note, a reduction of symmetry was detected when looking at the aromatic region in the $^{13}C\{^1H\}$ NMR spectra of chelates **1–9**. Thus, two sets of signals were observed for the *ipso-*, *ortho-*, *meta-*, and *para*-carbon atoms of the phenyl rings flanking the $Ph_2P–X–PPh_2$ ligands. Additionally, these resonances were split into multiplets due to $^{31}P–^{13}C$ coupling interactions.

The FT-IR spectra of complexes **1–9** were recorded in KBr pellets. In all cases, the most intense absorption was located around 1210 cm^{-1}. Another strong vibration was observed at *ca.* 1035 cm^{-1} (Table 2). Based on earlier experimental and computational studies,[29] these two bands were assigned, respectively, to the stretching of the C–OEt and C–S bonds within the xanthate anion. It should be pointed out that their actual wavenumbers suggested a significant contribution of the $EtO^+=CS_2^{2-}$ canonical form of the ligand, as further discussed below. Phenyl rings directly attached to a phosphorus atom in the $Ph_2P–X–PPh_2$ ligands gave rise to a characteristic sharp line at 1431 cm^{-1}. Other less informative absorptions observed on IR spectroscopy included weak C–H stretching vibration bands between 2800 and 3100 cm^{-1} for the various alkyl and aryl substituents of the xanthate and diphos ligands, as well as weak summation bands arising from combination and overtone of the aromatic C–H wagging vibrational modes between 1650 and 2000 cm^{-1}.

Table 2 IR stretching vibrations of the $[Ru(S_2COEt)_2(diphos)]$ chelates **1–9** (spectra recorded in KBr pellets)

Complex	ν PPh (cm^{-1})	ν CO (cm^{-1})	ν CS (cm^{-1})
$[Ru(S_2COEt)_2(dppm)]$ (**1**)	1430	1201	1039
$[Ru(S_2COEt)_2(dppe)]$ (**2**)	1432	1214	1034
$[Ru(S_2COEt)_2(dppp)]$ (**3**)	1430	1214	1036
$[Ru(S_2COEt)_2(dppb)]$ (**4**)	1431	1211	1036
$[Ru(S_2COEt)_2(dpppe)]$ (**5**)	1431	1217	1037
$[Ru(S_2COEt)_2(dppen]$ (**6**)	1431	1214	1034
$[Ru(S_2COEt)_2(dppbz)]$ (**7**)	1431	1217	1035
$[Ru(S_2COEt)_2(dppf)]$ (**8**)	1431	1215	1038
$[Ru(S_2COEt)_2(DPEphos)]$ (**9**)	1431	1209	1039

View Article Online
DOI: 10.1039/C8DT02838A

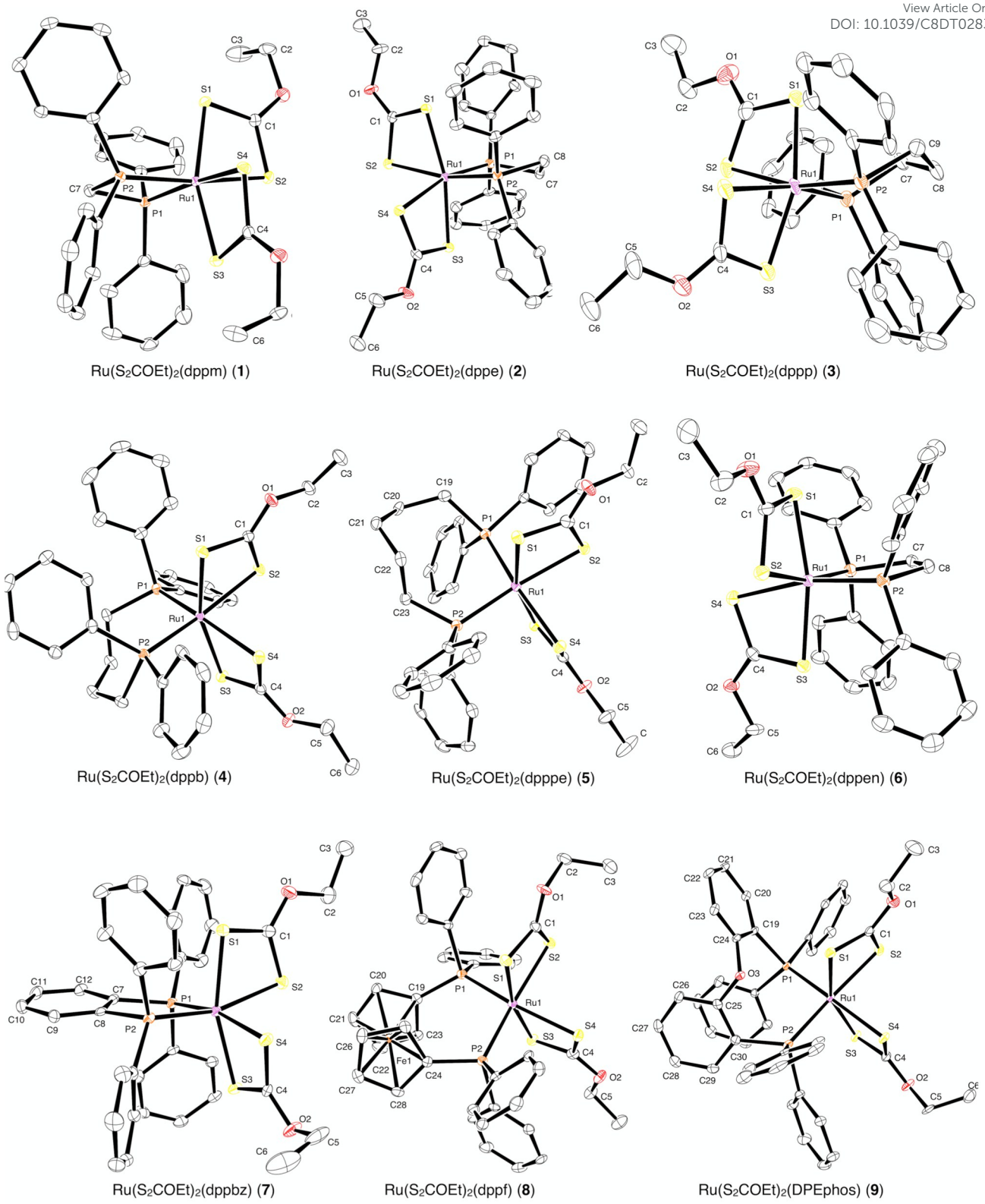

Fig. 1 ORTEP representations of [Ru(S$_2$COEt)$_2$(diphos)] complexes **1–9** (ellipsoids drawn at the 50% probability level). Co-crystallized solvent molecules and hydrogen atoms were omitted for clarity.

Dark yellow-brown crystals of complexes **1–9** suitable for X-ray diffraction analysis were easily obtained by slow evaporation of the mother liquors left after work-up (Fig. 1). Compounds **1**, **4**, **5**, and **7–9** crystallized as racemates in the monoclinic or triclinic lattice system. Racemic crystals of chelate **3** contained a co-crystallized CH_2Cl_2 molecule and belonged to the orthorhombic system. Only the Λ enantiomer of [Ru(S$_2$COEt)$_2$(dppe)] (**2**) and the Δ enantiomer of

View Article Online DOI: 10.1039/C8DT02678J

$[Ru(S_2COEt)_2(dppen)]$ (**6**) were present in the samples that we analyzed and they both crystallized in the orthorhombic $P2_12_12_1$ space group. Mononuclear entities featuring a highly distorted octahedral geometry around the metal center were observed in all cases (Chart 3). The two xanthate anions coordinated the ruthenium atom in a bidentate manner and displayed similar metrics. Likewise, the two phosphorus atoms of the diphosphine ligands were almost equivalent. Hence, only selected bond lengths and angles pertaining to half the coordination sphere of complexes **1**–**9** are listed in Table 3.

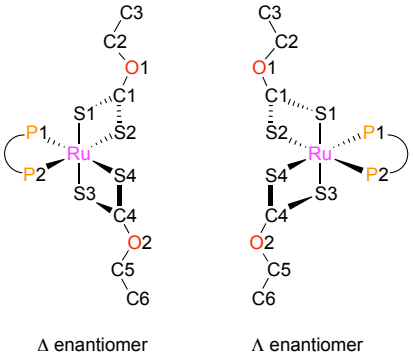

Chart 3 Topology of the Δ and Λ enantiomers of $[Ru(S_2COEt)_2(diphos)]$ chelates **1**–**9** showing the atom numbering system used for XRD analysis.

The Ru–P distances in complexes **1**–**5** that contained a phosphorus atom substituted by two phenyl groups and an alkyl chain varied between 2.25 and 2.32 Å (Table 3). Slightly shorter values (2.24 Å) were recorded for complexes **6** and **7** with an ethylene or an *ortho*-phenylene bridge, whereas compounds **8** and **9** with a ferrocene or a diphenylether linker led to a *ca.* 2.31 Å length that matched the Ru–PPh_3 distance previously determined in various *cis*-$[Ru(S_2COR)_2(PPh_3)_2]$ complexes (R = Me, Et, ^{i}Pr).[30] As expected, the exact nature of the spacer between the two phosphorus atoms had a profound influence on the P–Ru–P angle, which varied between 73° (with dppm in **1**) and 103° (with dppf in **8**). Furthermore, the values recorded in this study were much closer to the ligand's preferred bite angles (also known as natural bite angles) than to the metal's own requirements (90°), thereby indicating that the steric constraints imposed by the diphosphine ligands dictated the actual geometry of the complexes.[31] At *ca.* 2.39 Å, the Ru–S(1) and Ru–S(3) distances were always shorter than their Ru–S(2) and Ru–S(4) counterparts, which reached 2.46 Å on average. This 0.07 Å difference clearly shows that a phosphine ligand gives rise to a greater *trans* effect than a sulfur-based dithiocarboxylate unit, in line with earlier observations made on *cis*-$[Ru(S_2COR)_2(PPh_3)_2]$ complexes.[30]

In all the chelates under investigation, the S–Ru–S bite angle was almost invariant and equal to 72° (Table 3). Such an acute angle was mainly responsible for the strong distortion from an ideal octahedral geometry observed in complexes **1**–**9** with a quadratic elongation around 1.03 and an angular variance comprised between 86 and 124.[32] Other ruthenium chelates based on NHC·CS_2 zwitterions[2,6,33] or dithiocarbamate anions[27c,27d,30b] shared this feature. At about 115°, the S–C–S bite angle of the *O*-ethylxanthate ligand was also typical of 1,1-dithiolate chelates. Assuming that sodium or potassium xanthates were valid models for the uncoordinated $ROCS_2^-$ anions (although substantial $M^{+\cdots}S^-$ interionic contacts are observed in their crystal structures) led to an average S–C–S angle of 125° for the free ligands.[14] Thus, a contraction of 10° occurred upon chelation. Conversely, comparison of the C–S distances measured within compounds **1**–**9** and in NaS_2COEt or KS_2COEt did not reveal any significant variation. An average value of 1.69 Å was obtained in all cases. This figure is almost halfway between the standard lengths reported for C=S double bonds (1.60 Å) and C–S single bonds (1.81 Å).[34] Likewise, the average C–O distance in $[Ru(S_2COEt)_2(diphos)]$ complexes (1.33 Å) was intermediate between common values reported for CO single and double bonds (1.45 Å and 1.21 Å, respectively).[34] Moreover, the deviation from planarity between S(1), S(2), C(1) and O(1) was very limited. Altogether, these metrics further support IR spectroscopy measurements that suggested a significant contribution of the $EtO^+{=}CS_2^{2-}$ resonance form for the *O*-ethylxanthate ligand in complexes **1**–**9**.

Examination of the molecular structures of complexes **1**–**9** clearly revealed that each phosphorus atom of their diphosphine ligand had a phenyl ring pointing toward the ethyl group of the nearest xanthate unit (Fig. 1). Such a spatial proximity was held responsible for the inequivalence of the methylene protons observed on ^{1}H NMR spectroscopy (*vide supra*). The largest chemical shift differences between the two diastereotopic protons of the $OCH_aH_bCH_3$ system were observed with dppe (**2**), dppp (**3**), and dppen (**6**) ($\Delta\delta$ = 0.13, 0.19, and 0.16 ppm, respectively). These three compounds

Table 3 Selected bond distances (Å) and angles (°) derived from the molecular structures of $[Ru(S_2COEt)_2(diphos)]$ complexes **1**–**9**[a]

Complex (diphos)	**1** (dppm)	**2** (dppe)	**3** (dppp)	**4** (dppb)	**5** (dpppe)	**6** (dppen)	**7** (dppbz)	**8** (dppf)	**9** (DPEphos)
Ru(1)–P(1)	2.268(1)	2.256(1)	2.265(2)	2.283(1)	2.315(1)	2.246(1)	2.244(1)	2.312(1)	2.302(1)
Ru(1)–S(1)	2.389 (1)	2.378(1)	2.407(2)	2.396(1)	2.416(1)	2.392(2)	2.384 (1)	2.399(1)	2.408(6)
Ru(1)–S(2)	2.451 (1)	2.491(1)	2.464(2)	2.457 (1)	2.452(1)	2.463(2)	2.462(1)	2.450(1)	2.420(1)
C(1)–S(1)	1.692(2)	1.681(4)	1.714(9)	1.691(2)	1.693(4)	1.696(4)	1.681(3)	1.686(4)	1.688(3)
C(1)–S(2)	1.697(2)	1.693(4)	1.665(9)	1.691(2)	1.678(4)	1.678(6)	1.694(4)	1.693(3)	1.687(2)
C(1)–O(1)	1.326(2)	1.342(5)	1.337(10)	1.331(2)	1.334(5)	1.339(6)	1.329(4)	1.329(4)	1.343(3)
P(1)–Ru(1)–P(2)	73.14(2)	85.88(4)	91.31(7)	94.89(2)	99.26(4)	84.62(5)	85.61(3)	103.32(3)	96.60(2)
S(1)–Ru(1)–S(2)	72.23(2)	71.65(4)	71.87(8)	71.63(2)	71.78(3)	72.13(5)	72.03(3)	71.73(3)	72.15(2)
S(1)–C(1)–S(2)	114.7(1)	115.4(2)	115.6(5)	114.2(1)	115.7(3)	116.1(3)	115.2(2)	114.5 (2)	114.8(1)
S(1)–C(1)–O(1)–C(2)	–9.5(3)	6.8(6)	179.0(7)	–178.6(1)	–172.8(3)	–178.0(4)	175.7(3)	–171.6(3)	4.2(3)

[a] See Fig. 1 for ORTEP plots and Chart 3 for atom labeling.

gave rise to two well-resolved doublets of quadruplet around 4 ppm with $^{2}J_{H,H}$ = –10.3 Hz and $^{3}J_{H,H}$ = 7.1 Hz. All the other chelates led to overlapping second-order multiplets with the exception of [Ru(S_2COEt)$_2$(DPEphos)] (**9**), which exhibited an almost unsplit quadruplet. Variable temperature NMR experiments were carried out on a solution of [Ru(S_2COEt)$_2$(dppp)] (**3**) in DMSO-d_6. A complete coalescence was not observed even when the sample was heated up to 150 °C, which indicates that the conformation of the methylene group is strongly locked by the neighboring phenyl ring. Of note, the complex did not show any sign of thermal decomposition at this temperature.

Cyclic voltammetry

Cyclic voltammograms of complexes **1**–**9** were recorded at 100 mV/s in a 0.1 M solution of tetrabutylammonium perchlorate (TBAP) in dichloromethane. They all featured characteristic, quasi-reversible waves for the Ru^{2+}/Ru^{3+} redox couple centered at a $E_{1/2}$ value comprised between 0.65 and 0.80 V *vs.* Ag/AgCl (Fig. 2 and Table 4). This half-wave potential was clearly dependent on the diphosphine ligand nature and increased according to the sequence: **8** (dppf) < **1** (dppm) < **9** (DEPphos) < **5** (dpppe) < **4** (dppb) < **3** (dppp) < **2** (dppe) < **7** (dppbz) < **6** (dppen). Except for [Ru(S_2COEt)$_2$(dppm)] (**1**), there was a reverse correlation between $E_{1/2}$ and the P(1)–Ru–P(2) angles determined by X-ray crystallography, which decreased from 103 to 73° following the order: **8** (dppf) > **5** (dpppe) > **9** (DPEphos) > **4** (dppb) > **3** (dppp) > **2** (dppe) > **7** (dpbz) > **6** (dppen) > **1** (dppm). Hence, if we exclude complex **1** for being "too constrained", a larger bite angle of the diphosphine ligand led to an easier oxidation of Ru^{2+} into Ru^{3+}, irrespective of the exact nature of the linker group between the two phosphorus atoms. These data emphasize the importance of steric effects on the electron-donating properties of diphosphine ligands. It is indeed well-established that the P–M–P angles in metal chelates with bidentate phosphines are often quite different from those recorded in complexes featuring two unidentate phosphines and that geometric constraints imposed by the linker group may result in significant electronic differences.[35] Furthermore, because Ru(III) is slightly smaller than Ru(II) (ionic radii of 0.68 *vs.* 0.73 Å, respectively),[36] oxidation should be more difficult to perform with the most crowded ligand systems, leading to higher $E_{1/2}$ values. It is also worth highlighting the progressive increase of the current densities $I_{p,ox}$ and $I_{p,red}$ with the number of methylene units and the corresponding larger P(1)–Ru–P(2) bite angle within homologous complexes **2**–**5**, although we don't have any rationale for this observation.

In addition to the main peaks assigned to the Ru^{2+}/Ru^{3+} couple, additional signals were detected in some instances. Thus, we observed the reduction of unidentified by-products at *E* values of 0.2–0.3 V on the reverse scan with complexes **1**, **3**, and **6** (Fig. 2). The reversible oxidation of these compounds became visible around *E* = 0.3–0.4 V upon further cycling (not shown). This electrochemical response was not detected when the potential was cycled below 1.20 V. It most likely originates from the redox chemistry of dppm, dppp, and dppen, and specifically from an oxidation process that these ligands undergo when cycled above 1.20 V. A similar phenomenon was observed by Wilton-Ely and coworkers with bimetallic Ru(II) complexes bearing xanthate and dppm ligands.[37] Only for chelate **1** were additional peaks due to the Ru^{3+}/Ru^{4+} couple visible at $E_{1/2}$ = 1.15 V (Fig. 2), in line with earlier literature data.[25] Last but not least, the redox chemistry of ferrocene was highlighted from the cyclic voltammogram of [Ru(S_2COEt)$_2$(dppf)] (**8**). The Fe^{2+}/Fe^{3+} couple gave rise to a half-wave potential of 1.06 V. Similar values were already reported for complexes of the [RuCl_2(N–N)(dppf)] type (where N–N designates bipyridine or phenanthroline ligands).[38] Of note, the $E_{1/2}$ value for the free 1,1'-bis(diphenylphosphino)-ferrocene in TBAP/CH_2Cl_2 electrolyte is 0.70 V *vs.* Ag/AgCl.[38b]

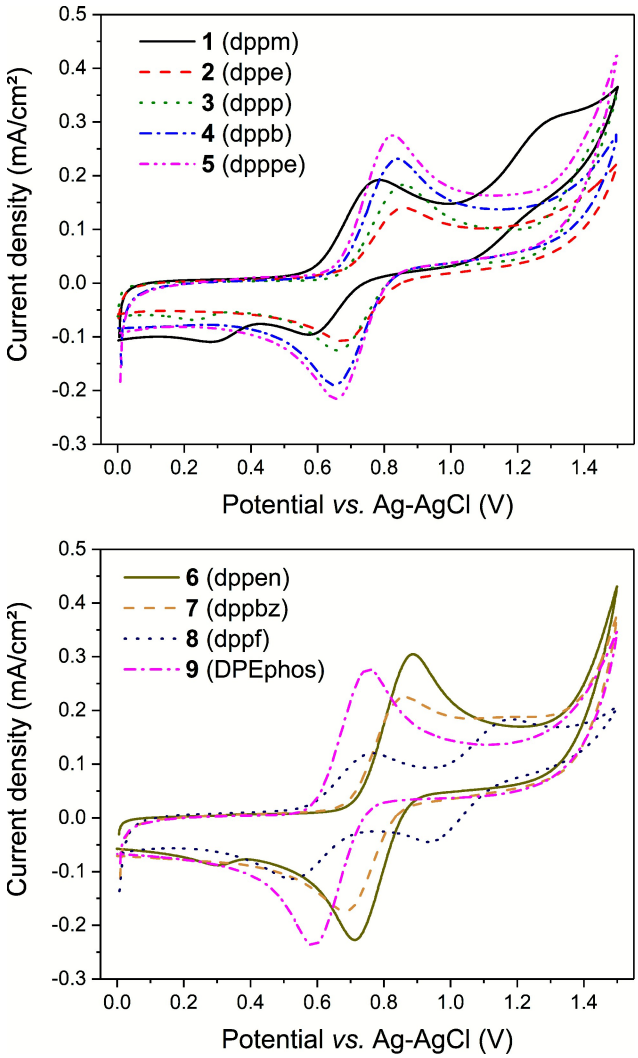

Fig. 2 Cyclic voltammograms of [Ru(S_2COEt)$_2$(diphos)] chelates **1**–**9** dissolved in 0.1 M TBAP/CH_2Cl_2 (only the first cycles are displayed).

View Article Online
DOI: 10.1039/C8DT02838A

Table 4 Half-wave potentials for the Ru^{2+}/Ru^{3+} redox couple determined by cyclic voltammetry[a] and diphosphine bite angle of complexes **1–9** determined by XRD

Complex	$E_{1/2}$ (V)	P(1)–Ru(1)–P(2) angle (°)
$[Ru(S_2COEt)_2(dppm)]$ (**1**)	0.668	73
$[Ru(S_2COEt)_2(dppe)]$ (**2**)	0.769	86
$[Ru(S_2COEt)_2(dppp)]$ (**3**)	0.759	91
$[Ru(S_2COEt)_2(dppb)]$ (**4**)	0.743	95
$[Ru(S_2COEt)_2(dpppe)]$ (**5**)	0.740	99
$[Ru(S_2COEt)_2(dppen]$ (**6**)	0.800	85
$[Ru(S_2COEt)_2(dppbz)]$ (**7**)	0.773	86
$[Ru(S_2COEt)_2(dppf)]$ (**8**)	0.645	103
$[Ru(S_2COEt)_2(DPEphos)]$ (**9**)	0.672	97

[a] Experimental conditions: TBAP in CH_2Cl_2 (0.1 M), Pt working and counter electrodes, Ag/AgCl reference electrode, room temperature, scan rate 100 mV/s.

Catalytic tests

Various types of ruthenium catalysts efficiently promote the formation of vinyl esters from benzoic acid and 1-hexyne with excellent selectivities toward either the branched product **10** or its (*E*) and (*Z*) linear isomers **11** and **12** (Table 5).[39] In particular, we devised a rapid and straightforward procedure for the regioselective synthesis of **10** using the readily available $[RuCl_2(p\text{-cymene})(PPh_3)]$ complex in toluene at 160 °C under microwave irradiation.[40] This experimental setup was adopted to probe the catalytic activity of $[Ru(S_2COEt)_2(diphos)]$ chelates **1–9** in the synthesis of enol esters. As shown in Table 5, low yields and poor selectivities were obtained in all cases. ^{31}P NMR analysis of the reaction media left after cooling, using a sealed capillary tube containing triphenylphosphine oxide in CD_2Cl_2 as an external reference (δ = 27.8 ppm), revealed that the starting complexes remained mostly unaltered, despite the harsh treatment that was applied to them. Only in the case of $[Ru(S_2COEt)_2(dppe)]$ (**2**) was a new singlet visible at δ = 43.7 ppm, while two small peaks located at δ = 41.8 and 0.6 ppm were detected with $[Ru(S_2COEt)_2(dppb)]$ (**4**) (Fig. S70).† These structural changes could explain the slightly better yields achieved with these two catalyst precursors compared with the other species examined, but we did not further investigate this possibility.

Table 5 Ruthenium-catalyzed synthesis of vinyl esters from benzoic acid and 1-hexyne[a]

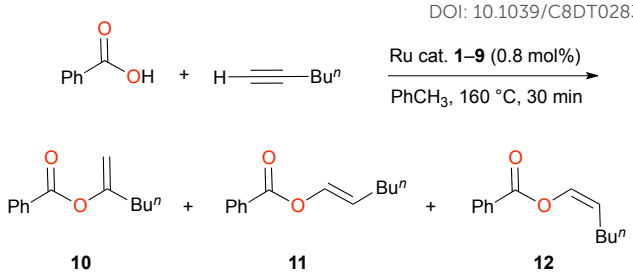

10 **11** **12**

Catalyst	Conversion (%)[b]	Selectivity (%)[b]		
		10	**11**	**12**
$[Ru(S_2COEt)_2(dppm)]$ (**1**)	2	42	24	34
$[Ru(S_2COEt)_2(dppe)]$ (**2**)	10	20	55	25
$[Ru(S_2COEt)_2(dppp)]$ (**3**)	3	34	19	47
$[Ru(S_2COEt)_2(dppb)]$ (**4**)	11	24	26	50
$[Ru(S_2COEt)_2(dpppe)]$ (**5**)	5	24	44	32
$[Ru(S_2COEt)_2(dppen]$ (**6**)	2	16	46	38
$[Ru(S_2COEt)_2(dppbz)]$ (**7**)	9	16	43	41
$[Ru(S_2COEt)_2(dppf)]$ (**8**)	11	27	29	44
$[Ru(S_2COEt)_2(DPEphos)]$ (**9**)	7	14	41	45

[a] Experimental conditions: catalyst (0.004 mmol), benzoic acid (0.5 mmol), 2.6 mL of a stock solution containing 1-hexyne (0.75 mmol) and isooctane (0.13 mmol) in dry toluene; microwave irradiation at 160 °C for 30 min. [b] Determined by GC using isooctane as an internal standard.

Next, we shifted our attention to the cyclopropanation of styrene with ethyl diazoacetate in the presence of chelates **1–9** (Table 6). This reaction is another representative catalytic process leading to highly valuable intermediates for organic synthesis, which greatly benefited from the intervention of ruthenium complexes, sometimes in an asymmetric fashion.[41] Our screening was carried out at 60 °C using 0.5 mol% of catalyst in the presence of air. The diazo compound was slowly added with a syringe pump over 5 h to minimize its unwanted dimerization. Despite this precaution, up to 10% of diethyl maleate and fumarate (**14**) were formed after a total reaction time of 50 h, as evidenced by GC analysis. Variations in the *cis/trans* ratio for these products were hardly meaningful and should not be overinterpreted. More importantly, the desired ethyl 2-phenylcyclopropanecarboxylate (**13**) was obtained in high yield (>90%) as a *ca.* 30/70 mixture of *cis* and *trans* isomers, irrespective of the exact nature of the diphosphine ligand. Monitoring the release of nitrogen with a gas burette throughout the reaction course confirmed that all the complexes under investigation behaved similarly and were rather slow promoters for the formal carbene insertion reaction (Fig. S71).† Indeed, it took them about 36 h to reach a quantitative consumption of ethyl diazoacetate. With the most efficient $[RuCl_2(p\text{-cymene})(NHC)]$ catalyst precursors, for instance, the reaction was complete in less than 6 h.[42]

Table 6 Ruthenium-catalyzed reactions of styrene and ethyl diazoacetate[a]

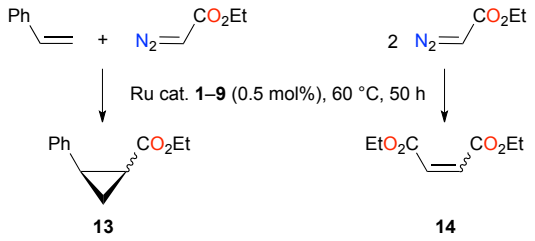

Catalyst	Cyclopropanes (**13**)		Dimers (**14**)	
	Yield (%)[b]	*Cis/trans* ratio[b]	Yield (%)[b]	*Cis/trans* ratio[b]
[Ru(S$_2$COEt)$_2$(dppm)] (**1**)	93	0.41	7	1.56
[Ru(S$_2$COEt)$_2$(dppe)] (**2**)	94	0.42	6	2.60
[Ru(S$_2$COEt)$_2$(dppp)] (**3**)	92	0.42	8	0.61
[Ru(S$_2$COEt)$_2$(dppb)] (**4**)	93	0.46	7	0.51
[Ru(S$_2$COEt)$_2$(dpppe)] (**5**)	94	0.47	6	1.41
[Ru(S$_2$COEt)$_2$(dppen] (**6**)	94	0.47	6	2.23
[Ru(S$_2$COEt)$_2$(dppbz)] (**7**)	92	0.43	8	0.49
[Ru(S$_2$COEt)$_2$(dppf)] (**8**)	93	0.44	7	0.91
[Ru(S$_2$COEt)$_2$(DPEphos)] (**9**)	90	0.45	10	1.63

[a] Experimental conditions: catalyst (0.005 mmol), styrene (2 mL), ethyl diazoacetate (1 mmol) diluted with styrene up to 1 mL and added in 5 h at 60 °C; 50 h total reaction time at 60 °C. [b] Determined by GC (relative errors are ± 5%).

Finally, we investigated the catalytic activity of complexes **1–9** in the atom transfer radical addition (ATRA) of carbon tetrachloride and methyl methacrylate (MMA). In this reaction, also known as the Kharasch addition, ruthenium acts as an halogen carrier in a reversible redox process.[43] Experiments were conducted in a monomodal microwave reactor at temperatures ranging between 100 and 160 °C (see the ESI for full details).† As we had demonstrated in 2007, such a device was very convenient to speed up the transformation by quickly bringing the reaction mixtures to temperatures well above the boiling points of the reagents and solvent.[44] In all the runs, the catalyst loading was 0.5 mol% and the halogen derivative was introduced in a fourfold excess compared to the olefin to ensure that only the mono- and diaddition products **15** and **16** were obtained, with no significant oligomerization or polymerization of MMA. Under these conditions, [Ru(S$_2$COEt)$_2$(dppm)] (**1**) emerged as the most potent catalyst at 140 °C (Table 7). Indeed, this complex afforded an almost complete conversion of MMA and a high selectivity toward the monoinsertion product **15**. When the temperature was raised to 160 °C, several other chelates became active and the proportion of product **16** increased significantly. ^{31}P NMR analysis of the reaction mixtures recovered after cooling, using a sealed capillary tube containing DMSO-d_6 for external lock, showed that only chelates **1** and **5** underwent significant alterations at 140 °C, in line with their greater catalytic activity. Evidence for the loss of diphosphine ligands from complexes **2**, **4**, **6**, and **8** became only visible at 160 °C, while species **3**, **7**, and **9** were even more robust (Fig. S73 and S74).† These results highlight the high thermal stability of compounds **1–9**, which is not surprising for 18-electron complexes bearing three strongly chelating ligands. Unlike other ruthenium catalysts for ATRA, such as the half-sandwich Ru(II) complex [Cp*RuCl(PPh$_3$)$_2$][45] or the related Ru(III) derivative [Cp*RuCl$_2$(PPh$_3$)] combined with magnesium as a reducing agent,[46] that were already active at 40 or 60 °C, the [Ru(S$_2$COEt)$_2$(diphos)] chelates displayed a latent behavior. With these compounds, formation of unsaturated active species occurred only above 100 °C and was most efficient with the dppm- and dppen-based complexes **1** and **5**, which feature, respectively, highly strained and rigid 4- and 5-membered diphosphinometallacycles. Hence, it can be assumed that active species were generated *via* partial or total decoordination of the diphosphine ligand rather than the xanthate ligands.

Table 7 Ruthenium-catalyzed atom transfer radical addition of carbon tetrachloride to methyl methacrylate[a]

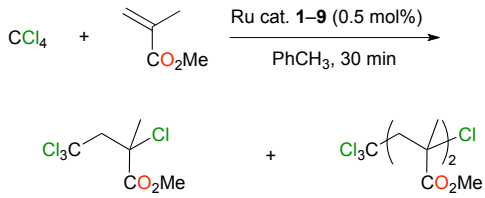

Catalyst	Reaction at 140 °C		Reaction at 160 °C	
	Yield (%)[b]	**15/16** ratio[b]	Yield (%)[b]	**15/16** ratio[b]
[Ru(S$_2$COEt)$_2$(dppm)] (**1**)	98	5.93	100	1.98
[Ru(S$_2$COEt)$_2$(dppe)] (**2**)	54	2.02	96	3.31
[Ru(S$_2$COEt)$_2$(dppp)] (**3**)	10	1.80	83	2.87
[Ru(S$_2$COEt)$_2$(dppb)] (**4**)	3	0.58	77	1.48
[Ru(S$_2$COEt)$_2$(dpppe)] (**5**)	81	1.97	83	1.40
[Ru(S$_2$COEt)$_2$(dppen] (**6**)	18	1.20	100	4.30
[Ru(S$_2$COEt)$_2$(dppbz)] (**7**)	4	0.89	60	2.26
[Ru(S$_2$COEt)$_2$(dppf)] (**8**)	2	0.43	50	1.24
[Ru(S$_2$COEt)$_2$(DPEphos)] (**9**)	5	0.80	47	1.28

[a] Experimental conditions: catalyst (0.006 mmol), 1.2 mL of a stock solution containing MMA (1.2 mmol), CCl$_4$ (4.8 mmol), and dodecane (0.18 mmol) in dry toluene; microwave irradiation at 140 °C or 160 °C for 30 min. [b] Determined by GC using dodecane as an internal standard.

Conclusions

The one-pot reaction of [RuCl$_2$(*p*-cymene)]$_2$ with potassium *O*-ethylxanthate and a set of nine representative diphosphine ligands was carried out in THF. Recourse to a monomodal microwave oven or a pressure reactor was found very convenient to shift equilibria toward the formation of monometallic [Ru(S$_2$COEt)$_2$(diphos)] chelates **1–9**, which were isolated in satisfactory to excellent yields after a simple work-up. All the products were fully characterized using various analytical techniques and their molecular structures were determined by X-ray diffraction analysis. In the solid state, they all featured a highly distorted octahedral geometry with a S–Ru–S bite angle close to 72° and P–Ru–P angles comprised between 73° and 103°, depending on the nature of the spacer group between the two phosphorus atoms. Bond lengths and IR stretching frequencies recorded for the anionic xanthate

ligands within complexes **1**–**9** strongly suggested a significant contribution of their $EtO^{+}=CS_2^{2-}$ resonance form. Moreover, ^{1}H NMR and XRD analyses showed that the methylene protons of the ethyl groups were diastereotopic and remained inequivalent even when the samples were heated up to 150 °C, due to a strong locking of their conformation by a neighboring phenyl ring on the diphos ligand. On cyclic voltammetry, quasi-reversible waves were observed for the Ru^{2+}/Ru^{3+} redox couple of the nine complexes under investigation. The $E_{1/2}$ values spanned the range comprised between 0.65 and 0.80 V *vs.* Ag/AgCl and could be correlated with the P(1)–Ru–P(2) bite angles of the diphosphine ligands determined by X-ray crystallography.

The activity of chelates **1**–**9** was probed in three different catalytic processes, namely, the synthesis of vinyl esters from benzoic acid and 1-hexyne, the cyclopropanation of styrene with ethyl diazoacetate, and the atom transfer radical addition of carbon tetrachloride and methyl methacrylate. Only low yields and poor selectivities were obtained in the first case. ^{31}P NMR analysis of the reaction mixtures showed that the starting complexes remained mostly unaltered under the experimental conditions adopted, despite the harsh thermal treatment that was applied to them. In the second case, quantitative conversions of ethyl diazoacetate were achieved within 50 h at 60 °C. Monitoring the rate of nitrogen evolution revealed, however, that all the catalysts screened behaved rather similarly and were slower initiators than other types of ruthenium complexes. In the ATRA of CCl_4 and MMA, $[Ru(S_2COEt)_2(dppm)]$ (**1**) was singled out as a very active and selective catalyst already at 140 °C. Contrastingly, most of the other complexes investigated in this study resisted degradation up to 160 °C and were only moderately active. Altogether, these results are in line with the high stability displayed by $[Ru(S_2COEt)_2(diphos)]$ complexes **1**–**9**. Indeed, these 18-electron species are strongly chelated by two xanthate ligands and one diphosphine. Hence, their potential to release unsaturated, catalytically active species should be rather limited.

Experimental

General information

Unless otherwise specified, all the syntheses were carried out under a dry nitrogen atmosphere using standard Schlenk techniques. Solvents were distilled from appropriate drying agents and deoxygenated prior to use. The $[RuCl_2(p\text{-cymene})]_2$ dimer[47] and the diphosphines dppm, dppp, dppb, dpppe, dppf, and DPEphos were purchased from Strem. Potassium *O*-ethyl dithiocarbonate and the diphosphines dppe, dppen, and dppbz were obtained from Aldrich. Reactions under pressure were carried out using a CEM Discover monomodal microwave oven or an Anton Paar Monowave 50 reactor. Petroleum ether refers to the fraction of boiling point 40–60 °C and was purchased from VWR. ^{1}H, ^{13}C, and ^{31}P NMR spectra were recorded at 298 K with a Bruker DRX 400 spectrometer operating at 400.13, 100.62, and 161.85 MHz, respectively. Chemical shifts are listed in parts per million downfield from TMS and are referenced from the solvent peaks or TMS for ^{1}H and ^{13}C. Assignments were established with the help of APT, COSY, HMBC, and HSQC sequences. Infrared spectra were recorded with a Bruker Equinox 55 FT-IR spectrometer. Electrospray mass spectra were obtained using a Micromass LCT Premier instrument. GC analyses were performed on a Varian Star 3400 CX gas chromatograph equipped with a RSLM-150 capillary column (25 m × 0.25 mm, 0.25 µm film thickness) and a flame ionization detector. Elemental analyses were carried out in the Laboratory of Pharmaceutical Chemistry at the University of Liege.

Synthesis of $[Ru(S_2COEt)_2(diphos)]$ complexes

A 20 mL Schlenk flask or a 10 mL pressure vial containing a magnetic stirring bar was charged with $[RuCl_2(p\text{-cymene})]_2$ (245 mg, 0.40 mmol), a diphosphine (0.88 mmol, 2.2 equiv.), potassium *O*-ethylxanthate (283 mg, 1.76 mmol, 4.4 equiv.), and THF (8 mL). The reaction mixture was stirred for 24 h at room temperature. It was then heated with stirring at 80–90 °C for 24 h in an oil bath or at 130 °C for 1 h using a pressure reactor. The color changed from red to yellow-orange. After cooling to room temperature, the reaction mixture was brought back to air. It was centrifuged for 5–10 min and filtered through Celite® to remove KCl and the excess of KS_2COEt. The solvent was removed under vacuum on a rotary evaporator. The residue was washed with petroleum ether (3 × 5 mL) and diethyl ether (2 × 5 mL) to remove *p*-cymene and the excess of diphosphine, respectively. The crude product was dissolved in dichloromethane (2–3 mL) and slowly poured into diethyl ether (20 mL) under vigorous stirring. The precipitate was separated from the supernatant solution and dried under high vacuum.

$[Ru(S_2COEt)_2(dppm)]$ (1). Yellow solid (560 mg, 96% yield). ^{1}H NMR (400 MHz, $CDCl_3$): δ = 1.24 (t, $^{3}J_{H,H}$ = 7.1 Hz, 6 H, CH_3 OEt), 4.21 – 4.51 (m, 4 H, CH_2 OEt), 4.92 (t, $^{2}J_{P,H}$ = 10.2 Hz, 2 H, CH_2 dppm), 7.13 – 7.28 (m, 6H, Ph dppm), 7.29 – 7.38 (m, 4H, Ph dppm), 7.38 – 7.50 (m, 6H, Ph dppm), 7.65 – 7.81 (m, 4H, Ph dppm) ppm. ^{13}C NMR (101 MHz, $CDCl_3$): δ = 14.0 (s, CH_3 OEt), 50.7 (t, $^{1}J_{P,C}$ = 21.6 Hz, CH_2 dppm), 66.1 (s, CH_2 OEt), 127.9 (t, $^{3}J_{P,C}$ = 4.8 Hz, *m*-CH_{ar} dppm), 128.6 (t, $^{3}J_{P,C}$ = 4.9 Hz, *m*-CH_{ar} dppm), 129.0 (s, *p*-CH_{ar} dppm), 130.1 (s, *p*-CH_{ar} dppm), 130.7 (t, $^{2}J_{P,C}$ = 5.1 Hz, *o*-CH_{ar} dppm), 132.2 (t, $^{2}J_{P,C}$ = 5.7 Hz, *o*-CH_{ar} dppm), 134.8 (t, $^{1}J_{P,C}$ = 17.7 Hz, *i*-C_{ar} dppm), 135.9 (t, $^{1}J_{P,C}$ = 19.0 Hz, *i*-C_{ar} dppm), 226.5 (s, S_2CO) ppm. ^{31}P NMR (162 MHz, $CDCl_3$): δ = 3.34 (s) ppm. IR (KBr): ν = 3047 (w), 2970 (w), 2916 (w), 1430 (m), 1284 (m), 1201 (s), 1155 (m), 1086 (m), 1039 (m), 737 (m), 720 (m), 697 (m), 537 (m), 509 (m) cm^{-1}. ESI-MS (CH_3CN): *m/z* calcd for $C_{31}H_{32}O_2P_2RuS_4$ ($[M]^{+}$), 727.97983; found, 727.97887. Calc. for $C_{31}H_{32}O_2P_2RuS_4$: C, 51.2; H, 4.4; S, 17.6%. Found: C, 51.3; H, 4.6; S, 17.2%.

$[Ru(S_2COEt)_2(dppe)]$ (2).‡ Yellow solid (562 mg, 95% yield). ^{1}H NMR (400 MHz, $CDCl_3$): δ = 1.15 (t, $^{3}J_{H,H}$ = 7.1 Hz, 6 H, CH_3 OEt), 2.40 – 2.62 (m, 2 H, CH_2 dppe), 2.79 – 3.05 (m, 2 H, CH_2 dppe), 4.08 (dq, $^{2}J_{H,H}$ = –10.3, $^{3}J_{H,H}$ = 7.1 Hz, 2 H, CH_2 OEt), 4.21 (dq, $^{2}J_{H,H}$ = –10.3, $^{3}J_{H,H}$ = 7.1 Hz, 2 H, CH_2 OEt), 7.08 – 7.25 (m, 10 H, Ph dppe), 7.32 – 7.46 (m, 6 H, Ph dppe), 7.68 – 7.83 (m, 4 H, Ph dppe) ppm. ^{13}C NMR (101 MHz, $CDCl_3$): δ = 14.0 (s, CH_3 OEt),

30.2 (dd, $^{1}J_{P,C}$ = 23.9 Hz, $^{2}J_{P,C}$ = 21.3 Hz, CH_2 dppe), 66.1 (s, CH_2 OEt), 127.2 (t, $^{3}J_{P,C}$ = 4.4 Hz, *m*-CH_{ar} dppe), 128.4 (s, *p*-CH_{ar} dppe), 128.5 (t, $^{3}J_{P,C}$ = 4.6 Hz, *m*-CH_{ar} dppe), 130.0 (s, *p*-CH_{ar} dppe), 130.9 (t, $^{2}J_{P,C}$ = 4.2 Hz, *o*-CH_{ar} dppe), 133.1 (t, $^{2}J_{P,C}$ = 4.9 Hz, *o*-CH_{ar} dppe), 135.1 – 136.2 (m, *i*-C_{ar} dppe), 226.5 (s, S_2CO) ppm. ^{31}P NMR (162 MHz, $CDCl_3$): δ = 76.61 (s) ppm. IR (KBr): ν = 3046 (w), 2980 (w), 2890 (w), 1432 (m), 1214 (s), 1100 (m), 1034 (m), 738 (m), 693 (m), 523 (m) cm^{-1}. ESI-MS (CH_3CN): *m/z* calcd for $C_{32}H_{34}O_2P_2RuS_4$ ($[M]^+$), 741.99548; found, 741.99518. Calc. for $C_{32}H_{34}O_2P_2RuS_4$: C, 51.8; H, 4.6; S, 17.3%. Found: C, 48.4; H, 4.4; S, 16.8%.

[Ru(S_2COEt)$_2$(dppp)] (3). Yellow solid (514 mg, 85% yield). ^{1}H NMR (400 MHz, CD_2Cl_2): δ = 1.28 (t, $^{3}J_{H,H}$ = 7.1 Hz, 6 H, CH_3 OEt), 1.84 – 2.06 (m, 2 H, $CH_2CH_2CH_2$ dppp), 2.06 – 2.22 (m, 2 H, PCH_2 dppp), 2.66 – 2.86 (m, 2 H, PCH_2 dppp), 4.16 (dq, $^{2}J_{H,H}$ = –10.3, $^{3}J_{H,H}$ = 7.1 Hz, 2 H, CH_2 OEt), 4.31 (dq, $^{2}J_{H,H}$ = –10.2, $^{3}J_{H,H}$ = 7.1 Hz, 2 H, CH_2 OEt), 7.10 – 7.23 (m, 4 H, Ph dppp), 7.23 – 7.47 (m, 16 H, Ph dppp) ppm. ^{13}C NMR (101 MHz, CD_2Cl_2): δ = 14.3 (s, CH_3 OEt), 20.6 (s, PCH_2CH_2 dppp), 29.8 (d, $^{1}J_{P,C}$ = 16.8 Hz, PCH_2 dppp), 30.0 (d, $^{1}J_{P,C}$ = 16.7 Hz, PCH_2 dppp), 66.7 (s, CH_2 OEt), 127.8 (t, $^{3}J_{P,C}$ = 4.4 Hz, *m*-CH_{ar} dppp), 128.2 (t, $^{3}J_{P,C}$ = 4.6 Hz, *m*-CH_{ar} dppp), 129.1 (s, *p*-CH_{ar} dppp), 129.8 (s, *p*-CH_{ar} dppp), 132.3 (t, $^{2}J_{P,C}$ = 4.1 Hz, *o*-CH_{ar} dppp), 134.0 (t, $^{2}J_{P,C}$ = 5.0 Hz, *o*-CH_{ar} dppp), 136.4 – 137.8 (m, *i*-C_{ar} dppp), 137.8 – 139.2 (m, *i*-C_{ar} dppp), 226.6 (s, S_2CO) ppm. ^{31}P NMR (162 MHz, CD_2Cl_2): δ = 37.17 (s) ppm. IR (KBr): ν = 3041 (w), 2980 (w), 2937 (w), 2859 (w), 1430 (m), 1214 (s), 1036 (m), 695 (m), 509 (m) cm^{-1}. ESI-MS (CH_3CN): *m/z* calcd for $C_{33}H_{36}O_2P_2RuS_4$ ($[M]^+$), 756.01116; found, 756.01125. Calc. for $C_{33}H_{36}O_2P_2RuS_4$: C, 52.4; H, 4.8; S, 17.0%. Found: C, 51.8; H, 4.9; S, 16.3%.

[Ru(S_2COEt)$_2$(dppb)] (4).‡ Yellow solid (591 mg, 96% yield). ^{1}H NMR (400 MHz, $CDCl_3$): δ = 1.24 (t, $^{3}J_{H,H}$ = 7.1 Hz, 6 H, CH_3 OEt), 1.38 – 1.56 (m, 2 H, PCH_2CH_2 dppb), 1.69 – 1.95 (m, 2 H, PCH_2CH_2 dppb), 2.59 – 2.87 (m, 4 H, PCH_2 dppb), 3.94 – 4.33 (m, 4 H, CH_2 OEt), 7.13 – 7.31 (m, 10 H, Ph dppb), 7.30 – 7.49 (m, 6 H, Ph dppb), 7.57 – 7.79 (m, 4 H, Ph dppb) ppm. ^{13}C NMR (101 MHz, $CDCl_3$): δ = 13.9 (s, CH_3 OEt), 24.1 (s, PCH_2CH_2 dppb), 31.7 (t, $^{1}J_{P,C}$ = 13.7 Hz, PCH_2 dppb), 65.8 (s, CH_2 OEt), 126.9 (t, $^{3}J_{P,C}$ = 4.2 Hz, *m*-CH_{ar} dppb), 127.88 (s, *p*-CH_{ar} dppb),127.94 (t, $^{3}J_{P,C}$ = 4.5 Hz, *m*-CH_{ar} dppb), 129.6 (s, *p*-CH_{ar} dppb), 130.9 (t, $^{2}J_{P,C}$ = 3.7 Hz, *o*-CH_{ar} dppb), 134.1 (t, $^{2}J_{P,C}$ = 4.8 Hz, *o*-CH_{ar} dppb), 136.4 – 137.9 (m, *i*-C_{ar} dppb), 139.8 – 141.2 (m, *i*-C_{ar} dppb), 226.2 (s, S_2CO) ppm. ^{31}P NMR (162 MHz, $CDCl_3$): δ = 45.18 (s) ppm. IR (KBr): ν = 3051 (w), 2981 (w), 2916 (w), 2849 (w), 1431 (m), 1211 (s), 1119 (m), 1036 (m), 693 (m), 515 (m) cm^{-1}. ESI-MS (CH_3CN): *m/z* calcd for $C_{34}H_{38}O_2P_2RuS_4$ ($[M]^+$), 770.02678; found, 770.02585. Calc. for $C_{34}H_{38}O_2P_2RuS_4$: C, 53.0; H, 5.0; S, 16.7%. Found: C, 53.2; H, 5.1; S, 15.8%.

[Ru(S_2COEt)$_2$(dpppe)] (5). Yellow solid (583 mg, 93% yield). ^{1}H NMR (400 MHz, $CDCl_3$): δ = 1.30 (t, $^{3}J_{H,H}$ = 7.1 Hz, 6 H, CH_3 OEt), 1.35 – 1.56 (m, 6 H, $PCH_2(CH_2)_3CH_2P$ dpppe), 2.51 – 2.54 (m, 4 H, PCH_2 dpppe), 4.03 – 4.38 (m, 4 H, CH_2 OEt), 7.19 – 7.44 (m, 16 H, Ph dpppe), 7.64 (t, $^{3}J_{H,H}$ = 8.1 Hz, 4 H, Ph dpppe) ppm. ^{13}C NMR (101 MHz, $CDCl_3$): δ = 13.9 (s, CH_3 OEt), 20.8 (s, $PCH_2CH_2CH_2$ dpppe), 26.6 (t, $^{2}J_{P,C}$ = 5.2 Hz, PCH_2CH_2 dpppe), 28.2 (t, $^{1}J_{P,C}$ = 12.8 Hz, PCH_2 dpppe), 65.8 (s, CH_2 OEt), 127.0 (t, $^{3}J_{P,C}$ = 4.1 Hz, *m*-CH_{ar} dpppe), 127.7 (t, $^{3}J_{P,C}$ = 4.5 Hz, *m*-CH_{ar} dpppe), 128.0 (s, *p*-CH_{ar} dpppe), 129.5 (s, *p*-CH_{ar} dpppe), 130.5 (t, $^{2}J_{P,C}$ = 3.5 Hz, *o*-CH_{ar} dpppe), 134.6 (t, $^{2}J_{P,C}$ = 5.1 Hz, *o*-CH_{ar} dpppe), 135.8 – 136.9 (m, *i*-C_{ar} dpppe), 141.7 – 142.6 (m, *i*-C_{ar} dpppe), 225.7 (s, S_2CO) ppm. ^{31}P NMR (162 MHz, $CDCl_3$): δ = 43.57 (s) ppm. IR (KBr): ν = 3049 (w), 2977 (m), 2924 (w), 2851 (w), 1431 (m), 1207 (s), 1121 (m), 1037 (m), 694 (m), 496 (m) cm^{-1}. ESI-MS (CH_3CN): *m/z* calcd for $C_{35}H_{40}O_2P_2RuS_4$ ($[M]^+$), 784.04243; found, 784.04124. Calc. for $C_{35}H_{40}O_2P_2RuS_4$: C, 53.6; H, 5.1; S, 16.4%. Found: C, 53.8; H, 5.3; S, 15.6%.

[Ru(S_2COEt)$_2$(dppen)] (6). Yellow solid (432 mg, 73% yield). ^{1}H NMR (400 MHz, $CDCl_3$): δ = 1.11 (t, $^{3}J_{H,H}$ = 7.1 Hz, 6 H, CH_3 OEt), 4.00 (dq, $^{2}J_{H,H}$ = –10.3, $^{3}J_{H,H}$ = 7.1 Hz, 2 H, CH_2 OEt), 4.16 (dq, $^{2}J_{H,H}$ = –10.3, $^{3}J_{H,H}$ = 7.1 Hz, 2 H, CH_2 OEt), 7.04 – 7.24 (m, 10 H, Ph dppen), 7.42 (m, 6 H, Ph dppen), 7.80 (m, 4 H, Ph dppen), 7.85 – 8.04 (m, 2 H, CH=CH dppen) ppm. ^{13}C NMR (101 MHz, $CDCl_3$): δ = 13.9 (s, CH_3 OEt), 66.1 (s, CH_2 OEt), 127.2 (t, $^{3}J_{P,C}$ = 4.6 Hz, *m*-CH_{ar} dppen), 128.60 (s, *p*-CH_{ar} dppen), 128.64 (t, $^{3}J_{P,C}$ = 4.6 Hz, *m*-CH_{ar} dppen), 130.2 (s, *p*-CH_{ar} dppen), 131.3 – 131.7 (m, *o*-CH_{ar} dppen), 132.9 – 133.3 (m, *o*-CH_{ar} dppen), 133.6 (dd, $^{1}J_{P,C}$ = 44.7, $^{4}J_{P,C}$ = 3.1 Hz, *i*-C_{ar} dppen), 134.6 (dd, $^{1}J_{P,C}$ = 45.9, $^{4}J_{P,C}$ = 3.4 Hz, *i*-C_{ar} dppen), 150.0 (dd, $^{1}J_{P,C}$ = 36.6, $^{2}J_{P,C}$ = 34.2 Hz, CH=CH dppen), 226.5 (s, S_2CO) ppm. ^{31}P NMR (162 MHz, $CDCl_3$): δ = 80.83 (s) ppm. IR (KBr): ν = 3043 (w), 2980 (w), 2420 (w), 2380 (w), 1431 (m), 1217 (s), 1094 (m), 1034 (m), 737 (m), 693 (m), 553 (m) cm^{-1}. ESI-MS (CH_3CN): *m/z* calcd for $C_{32}H_{32}O_2P_2RuS_4$ ($[M]^+$), 739.98044; found, 739.98105. Calc. for $C_{32}H_{32}O_2P_2RuS_4$: C, 52.0; H, 4.4; S, 17.3%. Found: C, 52.1; H, 4.6; S, 17.1%.

[Ru(S_2COEt)$_2$(dppbz)] (7). Yellow solid (388 mg, 62% yield). ^{1}H NMR (400 MHz, $CDCl_3$): δ = 1.15 (t, $^{3}J_{H,H}$ = 7.1 Hz, 6 H, CH_3 OEt), 4.03 – 4.32 (m, 4 H, CH_2 OEt), 7.12 – 7.22 (m, 4H, Ph dppbz), 7.22 – 7.29 (m, 6H, Ph dppbz), 7.32 – 7.41 (m, 6H, Ph dppbz), 7.42 – 7.50 (m, 2H, *m*-CH_{ar} C_6H_4 dppbz), 7.49 – 7.58 (m, 4H, Ph dppbz), 7.58 – 7.68 (m, 2H, *o*-CH_{ar} C_6H_4 dppbz) ppm. ^{13}C NMR (101 MHz, $CDCl_3$): δ = 14.0 (s, CH_3 OEt), 66.0 (s, CH_2 OEt), 127.1 (t, $^{3}J_{P,C}$ = 4.7 Hz, *m*-CH_{ar} Ph dppbz), 128.2 (t, $^{3}J_{P,C}$ = 4.7 Hz, *m*-CH_{ar} Ph dppbz), 128.8 (s, *p*-CH_{ar} Ph dppbz), 129.5 (s, *p*-CH_{ar} Ph dppbz), 130.0 (s, *m*-CH_{ar} C_6H_4 dppbz), 132.6 (dd, $^{2}J_{P,C}$ = 8.6, 4.5 Hz, *o*-CH_{ar} Ph dppbz), 133.0 (t, $^{2}J_{P,C}$ = 8.6 Hz, *o*-CH_{ar} C_6H_4 dppbz), 132.8 – 133.5 (m, *i*-C_{ar} Ph dppbz), 135.7 (dt, $^{1}J_{P,C}$ = 28.8 Hz, $^{4}J_{P,C}$ = 9.2 Hz, *i*-C_{ar} Ph dppbz), 146.6 (t, $J_{P,C}$ = 41.7 Hz, *i*-C_{ar} C_6H_4 dppbz), 226.4 (s, S_2CO) ppm. ^{31}P NMR (162 MHz, $CDCl_3$): δ = 78.39 (s) ppm. IR (KBr): ν = 3050 (w), 2980 (w), 2925 (w), 2852 (w), 1431 (m), 1217 (s), 1090 (m), 1035 (m), 693 (m), 557 (m), 528 (m) cm^{-1}. ESI-MS (CH_3CN): *m/z* calcd for $C_{36}H_{34}O_2P_2RuS_4$ ($[M]^+$), 789.99548; found, 789.99564. Calc. for $C_{36}H_{34}O_2P_2RuS_4$: C, 54.7; H, 4.3; S, 16.2%. Found: C, 54.6; H, 4.4; S, 15.9%.

[Ru(S_2COEt)$_2$(dppf)] (8). Yellow solid (638 mg, 89% yield). ^{1}H NMR (400 MHz, $CDCl_3$): δ = 1.19 (t, $^{3}J_{H,H}$ = 7.1 Hz, 6 H, CH_3 OEt), 4.05 – 4.20 (m, 4 H, CH_2 OEt), 4.23 (s, 2 H, Cp dppf), 4.35 (d, $^{3}J_{P,H}$ = 11.2 Hz, 4 H, Cp dppf), 4.51 (s, 2 H, Cp dppf), 7.18 – 7.38 (m, 12 H, Ph dppf), 7.49 – 7.74 (m, 8 H, Ph dppf) ppm. ^{13}C NMR (101 MHz, $CDCl_3$): δ = 13.9 (s, CH_3 OEt), 66.0 (s, CH_2 OEt), 70.6 (s, *m*-Cp dppf), 72.7 (t, $^{2}J_{P,C}$ = 3.2 Hz, *o*-Cp dppf), 74.0 (s, *m*-Cp dppf), 76.2 (t, $^{2}J_{P,C}$ = 7.0 Hz, *o*-Cp dppf), 83.0 ('dt', *N* = 61.7 Hz, *i*-Cp dppf),§ 126.6 (t, $^{3}J_{P,C}$ = 4.4 Hz, *m*-CH_{ar} Ph dppf), 127.3 (t,

View Article Online DOI: 10.1039/C8DT02838A

$^{3}J_{P,C}$ = 4.4 Hz, *m*-CH_{ar} Ph dppf), 128.7 (s, *p*-CH_{ar} Ph dppf), 129.2 (s, *p*-CH_{ar} Ph dppf), 134.0 (t, $^{2}J_{P,C}$ = 4.6 Hz, *o*-CH_{ar} Ph dppf), 134.6 (t, $^{2}J_{P,C}$ = 4.7 Hz, *o*-CH_{ar} Ph dppf), 134.9 ('dt', *N* = 58.4 Hz, *i*-C_{ar} Ph dppf),§ 138.1 ('dt', *N* = 64.4 Hz, *i*-C_{ar} Ph dppf),§ 225.0 (s, S_2CO) ppm. ^{31}P NMR (162 MHz, $CDCl_3$): δ = 46.68 (s) ppm. IR (KBr): ν = 3046 (w), 2973 (w), 2945 (w), 2899 (w), 1431 (m), 1215 (s), 1161 (m), 1038 (m), 696 (m) cm^{-1}. ESI-MS (CH_3CN): *m/z* calcd for $C_{40}H_{38}FeO_2P_2RuS_4$ ($[M]^+$), 897.96172; found, 897.96031. Calc. for $C_{40}H_{38}FeO_2P_2RuS_4$: C, 53.5; H, 4.3; S, 14.3%. Found: C, 52.8; H, 4.4; S, 13.8%.

[Ru(S_2COEt)$_2$(DPEphos)] (9). Yellow solid (654 mg, 93% yield). ^{1}H NMR (400 MHz, $CDCl_3$) δ = 1.19 (t, $^{3}J_{H,H}$ = 7.0 Hz, 6 H, CH_3 OEt), 3.96 – 4.43 (m, 4 H, CH_2 OEt), 6.60 – 7.62 (m, 28 H, Ph DPEphos) ppm. ^{13}C NMR (101 MHz, $CDCl_3$): δ = 13.9 (s, CH_3 OEt), 65.7 (s, CH_2 OEt), 123.3 (s, Ph), 126.2 – 126.5 (m, Ph), 127.2 – 127.7 (m, Ph), 128.4 (s, Ph), 129.0 (s, Ph), 130.7 (s, Ph), 133.6 (s, Ph), 133.9 (s, Ph), 159.4 (s, Ph), 224.9 (s, S_2CO) ppm. ^{31}P NMR (162 MHz, $CDCl_3$): δ = 43.45 (s) ppm. IR (KBr): ν = 3053 (w), 2981 (w), 2931 (w), 2888 (w), 1431 (m), 1209 (s), 1039 (m), 694 (m), 518 (m) cm^{-1}. ESI-MS (CH_3CN): *m/z* calcd for $C_{42}H_{38}O_3P_2RuS_4$ ($[M]^+$), 882.02170; found, 882.02064. Calc. for $C_{42}H_{38}O_3P_2RuS_4$: C, 57.2; H, 4.3; S, 14.5%. Found: C, 56.8; H, 4.4; S, 14.4%.

X-Ray crystallography

Crystals of [Ru(S_2COEt)$_2$(diphos)] complexes **1**–**9** suitable for XRD analysis were obtained by slow evaporation at –20 °C of the supernatant solutions left after the final precipitation from CH_2Cl_2/Et_2O. Data were collected on a Bruker APPEX II diffractometer using Mo-Kα radiation (λ = 0.71073 Å) from a fine focus sealed tube source at 100 K. Computing data and reduction was made with the APPEX II software.[48] Absorption corrections based on the multiscan method were applied.[49] All the structures were solved using SIR2004.[50] They were refined by full-matrix, least-squares based on F^2 using SHELXL.[51] An empirical absorption correction was applied using SADABS.[52] All non-hydrogen atoms were anisotropically refined and the hydrogen atom positions were calculated and refined using a riding model (see the ESI† for further information).

Cyclic voltammetry

Cyclic voltammograms were recorded at room temperature using a Biologic SP-200 potentiostat and a classical 3-electrode setup with 2 Pt foils of 1 cm² as working and counter electrodes and a REF361 Ag/AgCl reference electrode from Hach. Complexes **1**–**9** (10 mg each) were dissolved in a 0.1 M solution of (Bu_4N)(ClO_4) in dichloromethane (30 mL). After 10 min of degassing with N_2, CV curves were recorded between 0.0 and +1.5 V *vs.* Ag/AgCl at 100 mV/s (see the ESI† for further information).

Synthesis of vinyl esters

A 10 mL pressure vial containing a magnetic stirring bar was charged with a [Ru(S_2COEt)$_2$(diphos)] complex (0.004 mmol) and benzoic acid (61 mg, 0.5 mmol). The reactor was purged of air by applying five vacuum/nitrogen cycles before a stock solution (2.6 mL) containing 1-hexyne (0.75 mmol) and isooctane (0.13 mmol) in dry toluene was added. The vial was capped under nitrogen, heated to 160 °C (monitored by an IR sensor), and held at that temperature for 30 min in a CEM Discover instrument with a 170 W microwave power. After rapid air-cooling by the unit, the reaction mixture was analyzed by GC using isooctane as an internal standard.

Cyclopropanation of styrene

A 10 mL vial equipped with a magnetic stirring bar and a septum was charged with a [Ru(S_2COEt)$_2$(diphos)] complex (0.005 mmol) and styrene (2 mL). The mixture was stirred in an oil bath thermostated at 60 °C. Ethyl diazoacetate (120 ± 5 mg, 1 mmol) was diluted up to 1 mL with styrene in a 1 mL syringe. This solution was added dropwise to the reaction mixture in 5 h using a syringe pump. Stirring was maintained for an additional 45 h at 60 °C. The rate of nitrogen evolution was monitored with a water column connected to the reaction flask via the septum and a metallic cannula. After 50 h, the reaction mixture was analyzed by gas chromatography and its composition was established by comparison with authentic samples.

ATRA of carbon tetrachloride to methyl methacrylate

A 10 mL pressure vial containing a magnetic stirring bar was charged with a [Ru(S_2COEt)$_2$(diphos)] complex (0.006 mmol). The reactor was purged of air by applying five vacuum/nitrogen cycles before a stock solution (1.2 mL) containing methyl methacrylate (1 M), carbon tetrachloride (4 M), and dodecane (0.15 M) in dry toluene was added. The vial was capped with a septum under nitrogen, heated to a given temperature (monitored by an IR sensor) in a CEM Discover instrument, and held at that temperature for 30 min. After rapid air-cooling by the unit, the reaction mixture was analyzed by gas chromatography using dodecane as an internal standard.

Conflicts of interest

There are no conflicts to declare.

Acknowledgements

The authors would like to thank Dr Nicolas Smargiasso for the MS analyses and Mr Stéphane Luts for IR spectroscopy.

Notes and references

‡ For complexes **2** and **4**, [$RuCl_2$(*p*-cymene)]$_2$ (245 mg, 0.40 mmol) and KS_2COEt (283 mg, 1.76 mmol, 4.4 equiv.) were stirred for 24 h at room temperature in THF (8 mL) before adding dppe or dppb (0.88 mmol, 2.2 equiv.) and heating the mixture for 1 h at 130 °C. The work-up remained unchanged.

§ For a definition of the *N* parameter that expresses the shift difference in Hz between the outer lines of a higher order spectrum, see: H. Günther, *Angew. Chem. Int. Ed. Engl.*, 1971, **11**, 861–874. See also: C. Albrecht, S. Gauthier, J. Wolf, R. Scopelliti and K. Severin, *Eur. J. Inorg. Chem.*, 2009, 1003–1010.

1 L. Delaude, A. Demonceau and J. Wouters, *Eur. J. Inorg. Chem.*, 2009, 1882–1891.
2 L. Delaude, X. Sauvage, A. Demonceau and J. Wouters, *Organometallics*, 2009, **28**, 4056–4064.
3 L. Delaude, *Eur. J. Inorg. Chem.*, 2009, 1681–1699.
4 For early contributions to this field see: (*a*) L. L. Borer and J. V. Kong, *Inorg. Chim. Acta*, 1986, **122**, 145–148; (*b*) L. L. Borer, J. V. Kong, P. A. Keihl and D. M. Forkey, *Inorg. Chim. Acta*, 1987, **129**, 223–226.
5 T. F. Beltrán and L. Delaude, *J. Clust. Sci.*, 2017, **28**, 667–678.
6 S. Naeem, A. L. Thompson, A. J. P. White, L. Delaude and J. D. E. T. Wilton-Ely, *Dalton Trans.*, 2011, **40**, 3737–3747.
7 M. J. D. Champion, R. Solanki, L. Delaude, A. J. P. White and J. D. E. T. Wilton-Ely, *Dalton Trans.*, 2012, **41**, 12386–12394.
8 S. Naeem, L. Delaude, A. J. P. White and J. D. E. T. Wilton-Ely, *Inorg. Chem.*, 2010, **49**, 1784–1793.
9 T. F. Beltrán, G. Zaragoza and L. Delaude, *Dalton Trans.*, 2017, **46**, 1779–1788.
10 T. F. Beltrán, G. Zaragoza and L. Delaude, *Dalton Trans.*, 2016, **45**, 18346–18355.
11 (*a*) A. Neuba, J. Ortmeyer, D. D. Konieczna, G. Weigel, U. Florke, G. Henkel and R. Wilhelm, *RSC Adv.*, 2015, **5**, 9217–9220; (*b*) J. Ortmeyer, U. Flörke, R. Wilhelm, G. Henkel and A. Neuba, *Eur. J. Inorg. Chem.*, 2017, 3191–3197.
12 G. Hogarth, in *Progress in Inorganic Chemistry*, ed. K. D. Karlin, John Wiley & Sons, Hoboken, NJ, 2005, vol. 53, pp. 71–561.
13 (*a*) I. Haiduc, D. B. Sowerby and S.-F. Lu, *Polyhedron*, 1995, **14**, 3389–3472; (*b*) I. Haiduc and D. B. Sowerby, *Polyhedron*, 1996, **15**, 2469–2521; (*c*) I. Haiduc and L. Yoong Goh, *Coord. Chem. Rev.*, 2002, **224**, 151–170.
14 (*a*) E. R. T. Tiekink and G. Winter, *Rev. Inorg. Chem.*, 1992, **12**, 183–302; (*b*) E. R. T. Tiekink and I. Haiduc, in *Progress in Inorganic Chemistry*, ed. K. D. Karlin, John Wiley & Sons, Hoboken, NJ, 2005, vol. 54, pp. 127–319.
15 (*a*) D. Coucouvanis, in *Progress in Inorganic Chemistry*, ed. S. J. Lippard, John Wiley & Sons, Hoboken, NJ, 1970, vol. 11, pp. 233–371; (*b*) R. Eisenberg, in *Progress in Inorganic Chemistry*, ed. S. J. Lippard, John Wiley & Sons, Hoboken, NJ, 1970, vol. 12, pp. 295–369; (*c*) D. Coucouvanis, in *Progress in Inorganic Chemistry*, ed. S. J. Lippard, John Wiley & Sons, Hoboken, NJ, 1979, vol. 26, pp. 301–469; (*d*) R. P. Burns, F. P. McCullough and C. A. McAuliffe, in *Advances in Inorganic Chemistry and Radiochemistry*, eds. H. J. Emeléus and A. G. Sharpe, Academic Press, New York, NY, 1980, vol. 23, pp. 211–280.
16 W. C. Zeise, *Ann. Chim. Phys.*, 1822, **21**, 160–178.
17 G. H. Harris, *Xanthates* in *Kirk-Othmer Encyclopedia of Chemical Technology*, Wiley, 2000.
18 E. M. Donaldson, *Talanta*, 1976, **23**, 417–426.
19 S. Z. Zard, *Angew. Chem. Int. Ed.*, 1997, **36**, 672–685.
20 F.-h. Wu, L. Chen, X.-f. Chu and X.-w. Wei, *Chem. Res. Chin. Univ.*, 2013, **29**, 574–578.
21 L. Delaude and A. Demonceau, *Dalton Trans.*, 2012, **41**, 9257–9268.
22 C. O'Connor, J. D. Gilbert and G. Wilkinson, *J. Chem. Soc. A*, 1969, 84–87.
23 P. B. Critchlow and S. D. Robinson, *J. Chem. Soc., Dalton Trans.*, 1975, 1367–1372.
24 N. Bag, G. K. Lahiri and A. Chakravorty, *J. Chem. Soc., Dalton Trans.*, 1990, 1557–1561.
25 L. Ballester, O. Esteban, A. Gutierrez, M. Felisa Perpiñan, C. Ruiz-Valero, E. Gutierrez-Puebla and M. Jesus Gonzalez, *Polyhedron*, 1992, **11**, 3173–3182.
26 For a few selected examples, see: (*a*) A. R. Katritzky, U. Gruntz, N. Mongelli and M. C. Rezende, *J. Chem. Soc., Perkin Trans. 1*, 1979, 1953–1956; (*b*) J. Torres-Murro, L. Quintero and F. Sartillo-Piscil, *Tetrahedron Lett.*, 2005, **46**, 7691–7694; (*c*) E. Abdel-Latif, *Phosphorus, Sulfur Silicon Relat. Elem.*, 2006, **181**, 125–139; (*d*) L. Jean-Baptiste, S. Yemets, R. Legay and T. Lequeux, *J. Org. Chem.*, 2006, **71**, 2352–2359; (*e*) L. J. Johnson, E. Khosravi, O. M. Musa, R. E. Simnett and A. M. Eissa, *J. Polym. Sci. Part A: Polym. Chem.*, 2015, **53**, 775–786; (*f*) M. Franz, T. Stalling, R. Schaper, M. Schmidtmann and J. Martens, *Synthesis*, 2017, **49**, 4045–4054.
27 For a few selected examples, see: (*a*) A. G. Alonso and L. B. Reventós, *J. Organomet. Chem.*, 1988, **338**, 249–254; (*b*) S. O. Pinheiro, J. R. de Sousa, M. O. Santiago, I. M. M. Carvalho, A. L. R. Silva, A. A. Batista, E. E. Castellano, J. Ellena, Í. S. Moreira and I. C. N. Diógenes, *Inorg. Chim. Acta*, 2006, **359**, 391–400; (*c*) S. Y. Ng, J. Tan, W. Y. Fan, W. K. Leong, L. Y. Goh and R. D. Webster, *Eur. J. Inorg. Chem.*, 2007, 3827–3840; (*d*) K. Santos, L. R. Dinelli, A. L. Bogado, L. A. Ramos, É. T. Cavalheiro, J. Ellena, E. E. Castellano and A. A. Batista, *Inorg. Chim. Acta*, 2015, **429**, 237–242.
28 O. Kühl, *Phosphorus-31 NMR Spectroscopy. A Concise Introduction for the Synthetic Organic and Organometallic Chemist*, Springer, Berlin, 2008, pp. 83–89.
29 (*a*) G. W. Watt and B. J. McCormick, *Spectrochim. Acta*, 1965, **21**, 753–761; (*b*) U. Agarwala, Lakshmi and P. B. Rao, *Inorg. Chim. Acta*, 1968, **2**, 337–339; (*c*) R. Mattes and G. Pauleickhoff, *Spectrochim. Acta, Part A*, 1974, **30**, 379–386.
30 (*a*) K. Noda, Y. Ohuchi, A. Hashimoto, M. Fujiki, S. Itoh, S. Iwatsuki, T. Noda, T. Suzuki, K. Kashiwabara and H. D. Takagi, *Inorg. Chem.*, 2006, **45**, 1349–1355; (*b*) F.-H. Wu, T. Duan, L. Lu, Q.-F. Zhang and W.-H. Leung, *J. Organomet. Chem.*, 2009, **694**, 3844–3851; (*c*) C. Valerio-Cárdenas, S. Hernández-Ortega, R. Reyes-Martínez and D. Morales-Morales, *Acta Crystallogr., Sect. E: Struct. Rep. Online*, 2013, **69**, m408–m409.
31 P. Dierkes and P. W. N. M. van Leeuwen, *J. Chem. Soc., Dalton Trans.*, 1999, 1519–1530.
32 For a definition of these parameters see: K. Robinson, G. V. Gibbs and P. H. Ribbe, *Science*, 1971, **172**, 567–570.
33 T. F. Beltrán, G. Zaragoza and L. Delaude, *Dalton Trans.*, 2017, **46**, 9036–9048.
34 F. H. Allen, D. G. Watson, L. Brammer, A. G. Orpen and R. Taylor, in *International Tables for Crystallography*, ed. E. Prince, Springer, Berlin, 2006, vol. C, pp. 790–811.
35 (*a*) L. F. Szczepura, J. Giambra, R. F. See, H. Lawson, T. S. Janik, A. J. Jircitano, M. R. Churchill and K. J. Takeuchi, *Inorg. Chim. Acta*, 1995, **239**, 77–85; (*b*) C. Crotti, E. Farnetti, T. Celestino, M. Stener and S. Fontana, *Organometallics*, 2004, **23**, 5219–5225; (*c*) C. Flener Lovitt, G. Frenking and G. S. Girolami, *Organometallics*, 2012, **31**, 4122–4132.
36 (*a*) R. D. Shannon, *Acta Crystallogr., Sect. A: Fundam. Crystallogr.*, 1976, **32**, 751–767; (*b*) F. A. Dunand, L. Helm and A. E. Merbach, in *Adv. Inorg. Chem*, eds. C. Hubbar and R. van Eldik, Elsevier, San Diego, 2003, vol. 54, p. 25.
37 Y. H. Lin, N. H. Leung, K. B. Holt, A. L. Thompson and J. D. E. T. Wilton-Ely, *Dalton Trans.*, 2009, 7891–7901.
38 (*a*) T. F. Gallatti, A. L. Bogado, G. V. Poelhsitz, J. Ellena, E. E. Castellano, A. A. Batista and M. P. de Araujo, *J. Organomet. Chem.*, 2007, **692**, 5447–5452; (*b*) P. Appelt, J. P. da Silva, O. Fuganti, L. E. N. Aquino, B. Sandrino, K. Wohnrath, V. A. Q. Santos, M. A. A. Cunha, A. Veiga, F. S. Murakami, D. F. Back and M. P. de Araujo, *J. Organomet. Chem.*, 2017, **846**, 326–334.
39 For a few selected examples, see: (*a*) L. J. Goossen, J. Paetzold and D. Koley, *Chem. Commun.*, 2003, 706–707; (*b*) F. Nicks, R. Aznar, D. Sainz, G. Muller and A. Demonceau, *Eur. J. Org. Chem.*, 2009, 5020–5027; (*c*) M. Nishiumi, H. Miura, K. Wada, S. Hosokawa and M. Inoue, *ACS Catal.*, 2012, **2**, 1753–1759; (*d*) K.-C. Cheung, W.-L. Wong, M.-H. So, Z.-Y. Zhou, S.-C. Yan and K.-Y. Wong, *Chem. Commun.*, 2013, **49**, 710–712; (*e*) J. Jeschke, C. Gäbler and H. Lang, *J. Org. Chem.*, 2016, **81**, 476–484.

View Article Online
DOI: 10.1039/C8DT02838A

40 F. Nicks, L. Libert, L. Delaude and A. Demonceau, *Aust. J. Chem.*, 2009, **62**, 227–231.
41 For a few selected examples, see: (*a*) G. Maas, *Chem. Soc. Rev.*, 2004, **33**, 183–190; (*b*) G. A. Ardizzoia, S. Brenna, S. Durini and B. Therrien, *Organometallics*, 2012, **31**, 5427–5437; (*c*) D. Huber, P. G. A. Kumar, P. S. Pregosin, I. S. Mikhel and A. Mezzetti, *Helv. Chim. Acta*, 2006, **89**, 1696–1715; (*d*) A. Tudose, A. Demonceau and L. Delaude, *J. Organomet. Chem.*, 2006, **691**, 5356–5365; (*e*) A. Grabulosa, A. Mannu, A. Mezzetti and G. Muller, *J. Organomet. Chem.*, 2012, **696**, 4221–4228.
42 M. Méret, A. M. Maj, A. Demonceau and L. Delaude, *Monatsh. Chem.*, 2015, **146**, 1099–1105.
43 For a few selected references, see: (*a*) A. Richel, S. Delfosse, C. Cremasco, L. Delaude, A. Demonceau and A. F. Noels, *Tetrahedron Lett.*, 2003, **44**, 6011–6015; (*b*) J. Wolf, K. Thommes, O. Briel, R. Scopelliti and K. Severin, *Organometallics*, 2008, **27**, 4464–4474; (*c*) R. P. Nair, T. H. Kim and B. J. Frost, *Organometallics*, 2009, **28**, 4681–4688; (*d*) K. Parkhomenko, L. Barloy, J.-B. Sortais, J.-P. Djukic and M. Pfeffer, *Tetrahedron Lett.*, 2010, **51**, 822–825; (*e*) K. Severin, *Chimia*, 2012, **66**, 386–388.
44 Y. Borguet, A. Richel, S. Delfosse, A. Leclerc, L. Delaude and A. Demonceau, *Tetrahedron Lett.*, 2007, **48**, 6334–6338.
45 F. Simal, L. Wlodarczak, A. Demonceau and A. F. Noels, *Tetrahedron Lett.*, 2000, **41**, 6071–6074.
46 (*a*) K. Thommes, B. Içli, R. Scopelliti and K. Severin, *Chem. Eur. J.*, 2007, **13**, 6899–6907; (*b*) M. A. Fernández-Zúmel, K. Thommes, G. Kiefer, A. Sienkiewicz, K. Pierzchala and K. Severin, *Chem. Eur. J.*, 2009, **15**, 11601–11607.
47 M. A. Bennett and A. K. Smith, *J. Chem. Soc., Dalton Trans.*, 1974, 233–241.
48 Bruker, *APEX II, Bruker AXS Inc.*, Madison, WI, USA, 2004.
49 R. C. Clark and J. S. Reid, *Acta Crystallogr., Sect. A: Fundam. Crystallogr.*, 1995, **51**, 887–897.
50 M. C. Burla, R. Caliandro, M. Camalli, B. Carrozzini, G. L. Cascarano, L. De Caro, C. Giacovazzo, G. Polidori and R. Spagna, *J. Appl. Cryst.*, 2005, **38**, 381–388.
51 G. M. Sheldrick, *SHELX-97 (SHELXS 97 and SHELXL 97), Programs for Crystal Structure Analyses*, University of Göttingen, Göttingen (Germany), 1998.
52 G. M. Sheldrick, *SADABS, Programs for Scaling and Correction of Area Detection Data*, University of Göttingen, Göttingen (Germany), 1996.

View Article Online
DOI: 10.1039/C8DT02838A

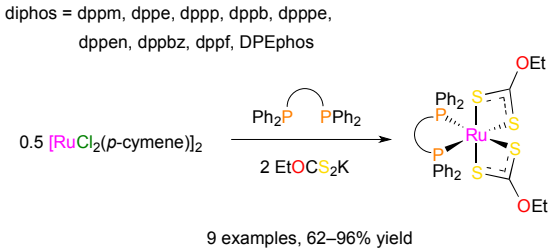

Nine ruthenium chelates with the generic formula [Ru(S_2COEt)$_2$(diphos)] were synthesized and fully characterized. Their catalytic activity was probed in three distinct reactions.